Progress In Electromagnetics Research C, Vol. 120, 45–60, 2022

UWB Filtenna with Reconfigurable and Sharp Dual-Band Notches for Underlay Cognitive Radio Applications

Yousif M. Hasan[1, *], Abdulkareem S. Abdullah[2], and Falih M. Alnahwi[2]

Abstract—In this paper, a compact UWB antenna with a reconfigurable and sharp dual-band notches filter to cancel the interference with some critical applications (5G WLAN, and X-band satellite downlink) is proposed for underlay cognitive radio (CR) applications. The dual notched bands are produced by coupling a pair of π-shaped resonators on both sides of the feed line and by etching a U-slot inside the feed line of the antenna. The proposed UWB filtenna in this configuration has a surface area of $22 \times 31\,\text{mm}^2$ and produces simulated (measured) reconfigurable notched frequencies at 5.466 GHz (5.7 GHz) and 7.578 GHz (7.44 GHz) with an impedance bandwidth of 3.024–10.87 GHz (2.825–10.74 GHz). Three PIN diodes are used to switch the presence of the dual-band notch. Two PIN diodes that turn ON-OFF simultaneously (D_{1A} & D_{1B}) are inserted within a pair of π-shaped resonators to control the 5G WLAN band notch, and a single diode (D_2) is embedded within a quarter wavelength resonator which is located inside the feed line of the antenna for controlling the X-band band notch. The simulation and measured results reveal that the proposed filtenna effectively covers UWB with controlled cancellation for interference with the intended bands. The realized gain is 4.5 dBi through the passband except in the notched frequencies, where it is decreased to less than -11 dBi in both notch frequencies. In other words, the proposed filtenna has a very high VSWR of greater than 20 at the notched frequencies.

1. INTRODUCTION

Since the Federal Communication Commission (FCC) approved commercial ultra-wideband (UWB) operation ranging from 3.1 to 10.6 GHz, this technology has fueled the interest of researchers [1, 2]. In the underlay cognitive radio, the unlicensed band 3.1–10.6 GHz for UWB allows a secondary user to use the spectrum of the licensed primary user but under a threshold power level [3]. Some critical applications do not allow any interference from secondary users, like the 5G WLAN operating range of (5.15–5.825) GHz [4, 5] and X-band satellite downlink operating range of (7.25–7.75) GHz that exist within the UWB [6]. Any interference with these critical applications leads to signal distortion and sensitivity loss [7]. Therefore, a UWB antenna must be designed to avoid interference with these critical applications [8, 9]. In the design process of UWB antennas, one should consider the following characteristics: compact size, low cost, high radiation efficiency, omnidirectional radiation patterns, and large bandwidth [10].

To utilize UWB for underlay cognitive radio, a notch band filter should be presented to reject undesired frequency bands. Several strategies can be used for band notch filtering, such as stepped impedance resonators (SIRs) [7], presenting special slots like those used by [11] and [12], capacitive loaded (CLL resonator) loop resonators [13], quarter and half wavelength parasitic elements [14] or stubs used in [15, 16], uniplanar Electromagnetic Band Gap (EBG) [17, 18], an arc slot etched on

Received 20 March 2022, Accepted 26 April 2022, Scheduled 6 May 2022

* Corresponding author: Yousif Mohsin Hasan (yousif.hasan@qu.edu.iq).

[1] Department of Electronic and Communication Engineering, College of Engineering, University of Al-Qadisiyah, Iraq. [2] Department of Electrical Engineering, College of Engineering, University of Basrah, Basrah, Iraq.

the patch antenna to produce half-wavelength resonator [19], and two pairs of EBGs and a single pair of split ring resonator (SRR) [20]. A few of these papers employ a reconfigurable notch band filter with the possibility of returning to a full UWB passband. In many of the works mentioned above, the notch band is permanent and cannot be removed. Some challenges, such as structural size, complex matching network, and high insertion loss, may flourish as a result of the (antenna and filter) combination [12, 21, 22]. These difficulties were considered when a compact filtenna was designed with a reconfigurable dual-band notch using PIN switching diodes to control the electromagnetic interference with two different critical applications.

In this work, two reconfigurable bandstop filters are integrated with a compact UWB antenna to minimize interference at 5G WLAN and X-band. Three PIN diodes are attached to the proposed filter to switch the two critical applications' cancelation. As mentioned in previous works, the disadvantage of using such reconfigurable antennas is the distortion in the radiation pattern of the antenna due to the attachment of the diodes and the biasing lines on the antenna patch. The filtenna system uses filter/antenna technology, which consists of a filter incorporated within the feed line of the antenna structure and holding the switching components to achieve a specific band operation, such as in [23–25]. The purpose of using the filtenna is to avoid etching and putting diodes on the antenna radiation patch element. A pair of half-wavelength π-shaped resonators are coupled on both sides of the feed line to produce the first notch band at 5.5 GHz. The second notch band at 7.6 GHz is created by etching a U-slot inside the antenna's feed line. The proposed filtenna has four modes depending on the status of the three PIN diodes, such as a fully covered UWB passband mode without notches, UWB with a single band notch mode at 5.5 GHz, UWB with a single band notch mode at 7.6 GHz, and UWB with a dual-band notch mode at 5.5 and 7.6 GHz. The generated band notches are sharp so that the VSWR is greater than 20 at the center frequency of the notched band.

This paper can be divided into sections. In Section 2, the proposed filtenna structure is introduced along with the necessary design steps. The simulation and measurement results are discussed in Section 3. The main conclusions extracted from this paper are presented in Section 4.

2. PROPOSED FILTENNA STRUCTURE

The proposed reconfigurable UWB filtenna is based on the following characteristics: passband (3.1–10.6) GHz, a center frequency of 5.73 GHz, feed line characteristic impedance of 50 Ω, and dual-band notches to cancel the interference with 5G WLAN and X-band satellite downlink. A reconfigurable dual notch band filter is integrated with the proposed UWB antenna to achieve the reconfigurable UWB filtenna as shown in Figure 1.

Figure 2 shows the structure and all dimensions of the reconfigurable UWB filtenna as well as the position of the PIN diodes (D_{1A}, D_{1B}, and D_2). The dielectric substrate of the antenna system is Rogers RT 5880 with a dielectric constant ϵ_r of 2.2, loss tangent of 0.009, and height h of 0.8 mm. The final parameter values of the proposed UWB filtenna are given in Table 1.

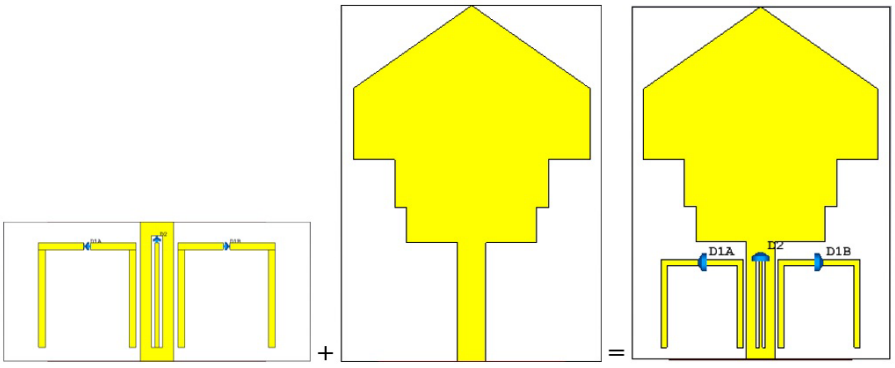

Figure 1. Schematics of (a) reconfigurable bandstop filter, (b) UWB antenna, (c) reconfigurable UWB filtenna.

Table 1. Best parameters values of the proposed filtenna.

Parameter	W_s	L_s	W_1	L_1	W_2	L_2	W_3	L_3	L_n
Values (mm)	22	31	11	3	13	4	20	6	7
Parameter	W_f	L_4	L_f	$u = L_5$	W_5	L_g	W_{stub}	L_{stub}	W_n
Values (mm)	2.4	7	11	2	2.5	10	0.4	7.5	0.5

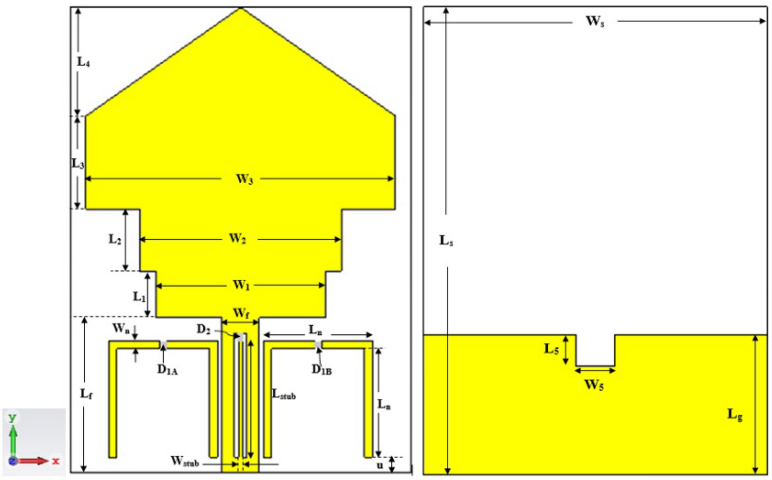

Figure 2. Proposed UWB filtenna structure, (a) front view, (b) back view.

2.1. Analysis of the Monopole UWB Antenna

Microstrip feed line, coplanar waveguide feed, aperture coupling feed, and proximity coupling feed are all options for feeding UWB monopole antennas [26]. Microstrip feed line is the feeding technology used in this work for constructing the UWB antenna. The antenna should have a characteristic impedance that satisfies the system's requirements. The width of the feed line of the UWB antenna was selected to be 2.4 mm to achieve a characteristic impedance of 50 Ω. The size of the radiating element determines the frequency of the first resonant mode. The antenna acts as a quarter-wavelength monopole antenna at the first resonance frequency (f_1). As a result, at the first resonance frequency, the length of the entire radiating element is a quarter wavelength ($\lambda/4$). The second (f_2) and third (f_3) modes are the harmonics of the fundamental mode. The total length of the radiating element (L) and the frequency of the fundamental mode (f_1) are calculated as:

$$L = L_1 + L_2 + L_3 + L_4 \tag{1}$$

$$f_1 = \frac{c}{4 \times L} \tag{2}$$

where c is the speed of light in free space. As given in [27, 28] and after the optimization process as shown in Figure 3, the width of the first part of the patch (W_1) that is connected to the transmission feed line is approximately equal to half the width of the ground plane (W_s) as given in Equation (3):

$$W_1 = \frac{W_s}{2} \tag{3}$$

The total length of the patch elements can be calculated using Equation (1) and found to be $L = 20$ mm, and then the first resonant frequency can be calculated using Equation (2) which is equal to $f_1 = 3.75$ GHz. From the simulated results of the reflection coefficient of the proposed antenna shown in Figure 4, the first resonant frequency is $f_1 = 3.53$ GHz, which is nearly equal to the predicted value.

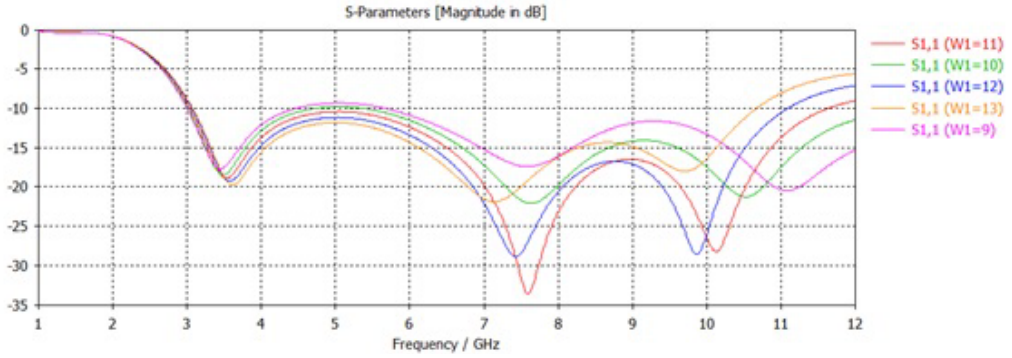

Figure 3. Simulated reflection coefficient of the proposed UWB antenna at different values of W_1.

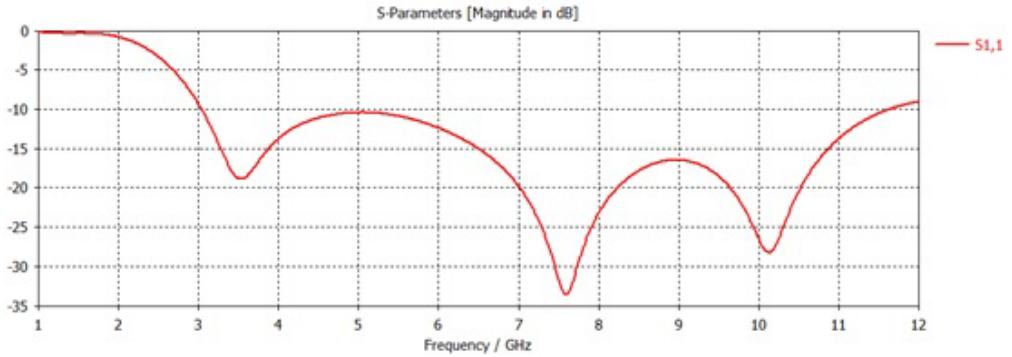

Figure 4. Simulated reflection coefficient of the proposed UWB antenna alone.

In the design of UWB monopole antennas, the gap between the partial ground plane and the transmission feed line is a critical parameter. The impedance matching between the transmission feed line and the radiating element is affected by the gap width. There is a square slot in the ground plane with dimensions of $(L_5 \times W_5)$ to improve the impedance bandwidth. Most of the current flow in UWB monopole antennas is focused at the antenna perimeter such as the current in a wire antenna running along the perimeters of the antenna radiating elements. When the UWB antenna is designed, the first resonant frequency should be slightly higher than the lower band boundary. At the lowest frequency within the passband, the perimeter of the patch element is equal to one wavelength. This frequency should be lower than the first resonant frequency of the antenna impedance bandwidth. The perimeter P_{re} in mm of the patch element of the proposed UWB filtenna can be determined as:

$$P_{re} = (W_1 - W_f) + 2L_1 + (W_2 - W_1) + 2L_2 + (W_3 - W_2) + 2L_3 + 2\sqrt{\left(\frac{W_3}{2}\right)^2 + {L_4}^2} \tag{4}$$

The lower frequency of the filtenna bandwidth can be calculated using this relationship since the perimeter of the patch element is approximately equal to one guided wavelength of the average medium of radiation.

$$P_{re} = \lambda_g \tag{5}$$

The lower resonant frequency of the proposed antenna can be calculated as [27, 28]:

$$f_L = \frac{c}{P_{re} \times \sqrt{\epsilon_{eff}}} \tag{6}$$

where ϵ_{eff} is the effective permittivity of the dielectric substrate and given by [29]:

$$\epsilon_{eff} = \frac{\epsilon_r + 1}{2} + \frac{\epsilon_r - 1}{2}\left[1 + \frac{12h}{W}\right]^{-0.5} \tag{7}$$

In the proposed UWB antenna, the perimeter of the patch element is $P_{re} = 68.013\,\text{mm}$, then the calculated lower frequency using Equation (6) is found as $f_L = 3.051\,\text{GHz}$. From the simulation results of the reflection coefficient (S_{11}) shown in Figure 4, the lowest frequency in the passband is 3.04 GHz, which is nearly equal to the calculated value. Also, the reflection coefficient of the antenna has three resonant frequencies, fundamental mode and two harmonics, as given in Table 2.

Table 2. Fundamental and harmonic resonant frequencies of the proposed UWB antenna.

Resonant frequency (GHz)	$f_1 = 3.53$	$f_2 = 7.6$	$f_3 = 10.13$
S_{11} (dB)	-18.89	-33.56	-28.33

2.2. Reconfigurable Band Notch Filter

The proposed filtenna includes a $50\,\Omega$ microstrip line in the top layer and a partial defected ground in the bottom layer of the notch filter with dimensions of 9 mm $\times$22 mm. By inserting an identical pair of π-shaped parasitic-element resonators on both sides of the feed line of the UWB antenna, the interference with the 5G WLAN applications is eliminated. The length of the π-shaped parasitic element can determine the center frequency of the first band notch. The length is approximately equal to half the guided wavelength resonator ($\lambda_g/2$) at the center frequency of the first band notch (f_{notch1}). As a result, the total length of the π-shaped parasitic element (L_{notch}) can be calculated using the following equation:

$$L_{notch} = 3 \times L_n = \frac{\lambda_g}{2} = \frac{c}{2 \times f_{notch1}\sqrt{\epsilon_{eff}}} \tag{8}$$

where λ_g represents the guided wavelength at the notch frequency of 5.5 GHz.

The coupling of the pair of π-shaped resonators can be represented by the lumped-element circuit shown in Figure 5. Each half-wavelength π-shaped resonator is represented by an inductor L and a capacitor C in the equivalent lumped element circuit. The coupling gap between the transmission feed line and the π-shaped resonator can be represented by a j-inverter [26]. The equations given in [30] can be used to calculate the values of inductors and capacitors in the equivalent circuit. Advanced Design System 2021 (ADS) [31] is used to simulate the s parameters of the LC equivalent circuit as shown in Figure 6. After optimization, the values of each lumped element are ($L = 10\,\text{nH}$, $C = 0.5\,\text{pF}$), and j-inverter is $C_j = 0.05\,\text{pF}$. The results show a full-pass response except at one frequency of 5.513 GHz where a notched band is attained. This frequency reasonably coincides with the frequency band which has to be rejected. The reflection coefficient (S_{11}) and transmission coefficient (S_{12}) obtained at this frequency are -1.8×10^{-6} and $-95.5\,\text{dB}$, respectively. The high transmission coefficient rejection and low reflection coefficient are obtained at the notched frequency because the simulation results are taken for ideal lumped elements that do not have any losses of metal or substrate.

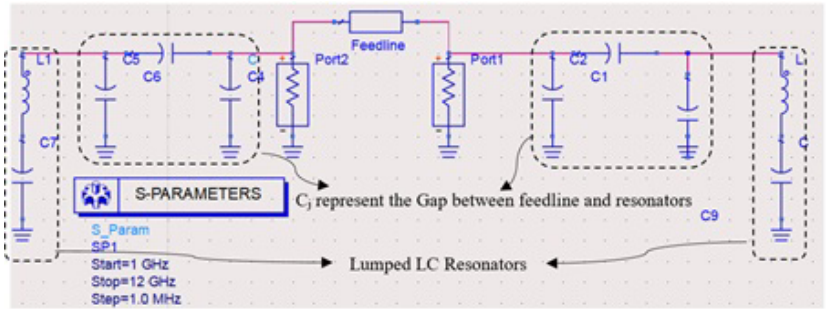

Figure 5. Equivalent lumped LC circuit of coupling a pair of π-shaped resonators.

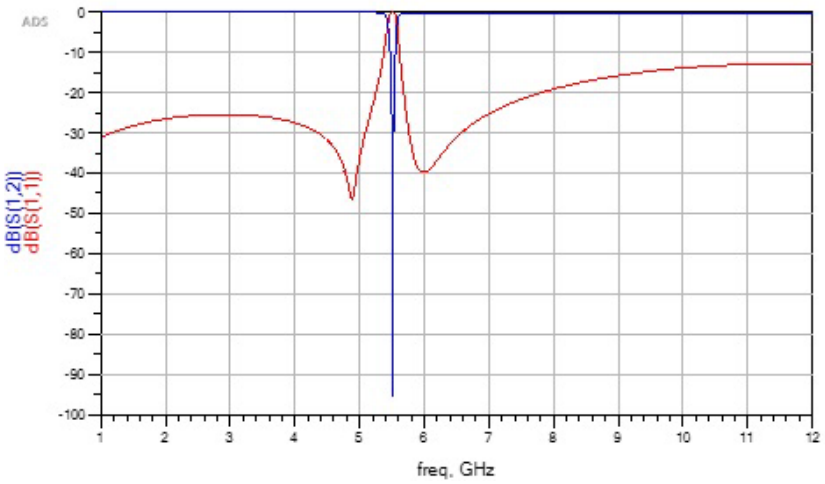

Figure 6. ADS simulated s-parameters of the LC equivalent circuit.

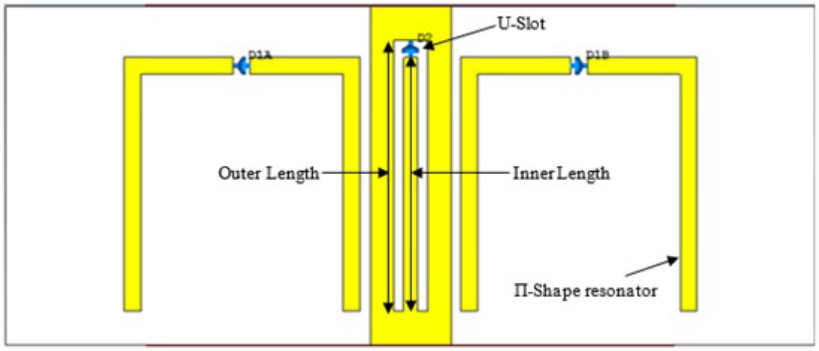

Figure 7. Structure of proposed reconfigurable bandstop filter as well as positions of PIN diodes.

A U-slot is etched on the feeding line of the antenna to eliminate the interference with the X-band satellite downlink as shown in Figure 7. The U-slot has an outer length of 8 mm and width of 1 mm, and it has an inner stub length of $L_{stub} = 7.5$ mm and width of $W_{stub} = 0.4$ mm. The inner length of the U-slot ensures that the filter has a fixed band notch [12]. The inner stub length (L_{stub}) is approximately equal to a quarter guided wavelength ($\lambda_g/4$) at center frequency of the second band notch ($f_{notch2} = 7.6$ GHz) and can be calculated as follows:

$$L_{stub} = \frac{\lambda_g}{4} = \frac{c}{4 \times f_{notch2}\sqrt{\epsilon_{eff}}} \tag{9}$$

The proposed dual notch band filter is simulated using CST Microwave Studio [32]. As shown in Figure 8, the simulated s-parameters of the filter have a UWB passband except for the dual notch frequencies. These frequencies are at 5.429 GHz and 7.627 GHz, which are almost the same as the frequency bands that have to be rejected.

Figure 9 illustrates the simulated surface current of the proposed stopband filter. The results were taken at the two notched frequencies 5.429 GHz and 7.627 GHz. Figure 9(a) depicts how the current is concentrated at the pair of π-shaped resonators at 5.429 GHz, which cancels out interference with the 5G WLAN bands. Furthermore, the current is centered around the quarter-wavelength resonator located inside the filter's feed line, and no current is passing from port 1 to port 2 at a frequency of 7.627 GHz, as shown in Figure 9(b), which indicates the presence of a stopband at 7.627 GHz.

To achieve a reconfigurable band notch filter behavior, a pair of PIN diodes that are turned ON-OFF simultaneously (D_{1A} and D_{1B}) are attached within each of the π-shaped resonators, and one PIN

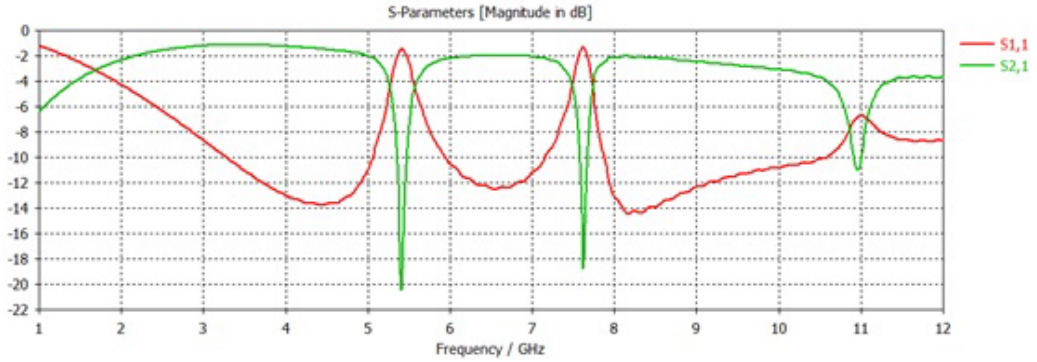

Figure 8. Simulated s-parameters of the proposed stopband filter.

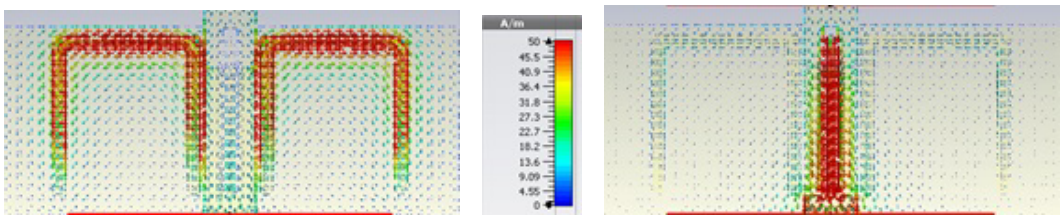

(a) (b)

Figure 9. Simulated surface current of the proposed stopband filter at (a) 5.429 GHz, (b) 7.627 GHz.

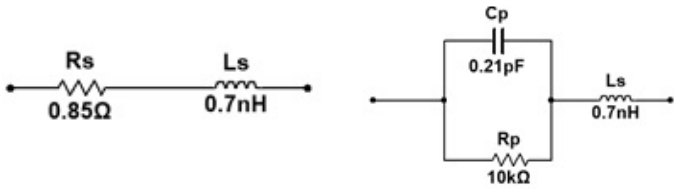

(a) (b)

Figure 10. Equivalent circuit of PIN diodes, (a) ON state and (b) OFF state.

diode (D_2) is combined within the inner stub length of the U-slot. As shown in Figure 10(a), a forward resistor R_s in series with a series inductor L_s can simulate the ON state equivalent circuit of a PIN diode (forward biasing). The diode OFF state (reverse biasing) can be modeled as a capacitor C_p in parallel with a large value resistor R_p, both in series with an inductor L_s, as shown in Figure 10(b). In this paper, a (SMP1340-079LF) PIN diode is utilized with $R_s = 0.85\,\Omega$ at 10 mA, $C_p = 0.21$ pF, and $L_s = 0.7$ nH [33].

3. THE SIMULATION AND MEASUREMENT RESULTS

Figures 11(a) and (b) show the front and back views, respectively, of the prototype of the proposed UWB filtenna. Measurements have been made using Vector Network Analyzer (Anritsu MS4642A-20 GHz) package. A pair of PIN diodes (D_{1A} and D_{1B}) are inserted at the locations given in Figure 7 which effectively divide each of the two single resonators of the π-shaped parasitic elements into two equal length segments. A 100 pF DC blocking capacitor (C) was inserted in the inner length of the U-slot to create the RF connection of the PIN diode and to isolate the RF signal from the DC for supplying the DC voltage to the PIN diode (D_2). The results are simulated by using CST microwave studio. There are four states in this proposed filtenna depending on the status of three PIN diodes.

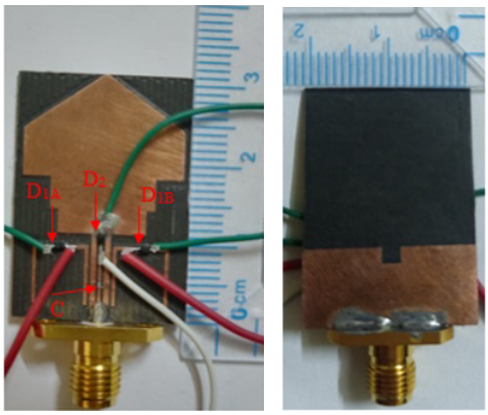

(a) (b)

Figure 11. Prototype filtenna, (a) front view, (b) back view.

3.1. State 1: (D_{1A} and D_{1B} are Turned OFF While D_2 Is Turned ON)

In this state, there is no notch band within the entire passband of the filtenna, so the resulting reflection coefficient of the filtenna covers the entire UWB spectrum. When the two PIN diodes are turned OFF, they act as insulators that cut the current flow in the pair of π-shaped resonators, resulting in the structure acting just like parallel transmission lines with no effect on the passband of the filtenna. When D_2 is turned ON, it acts as a conductor, and current flows inside the antenna feed line that completes the structure of the feed line without affecting the antenna passband (VSWR is less than 2 on the entire passband UWB). Figure 12(a) shows the simulated (measured) reflection coefficient of the filtenna whose coverage occupies the entire UWB range of 3.024–10.87 GHz (2.825–10.74 GHz)

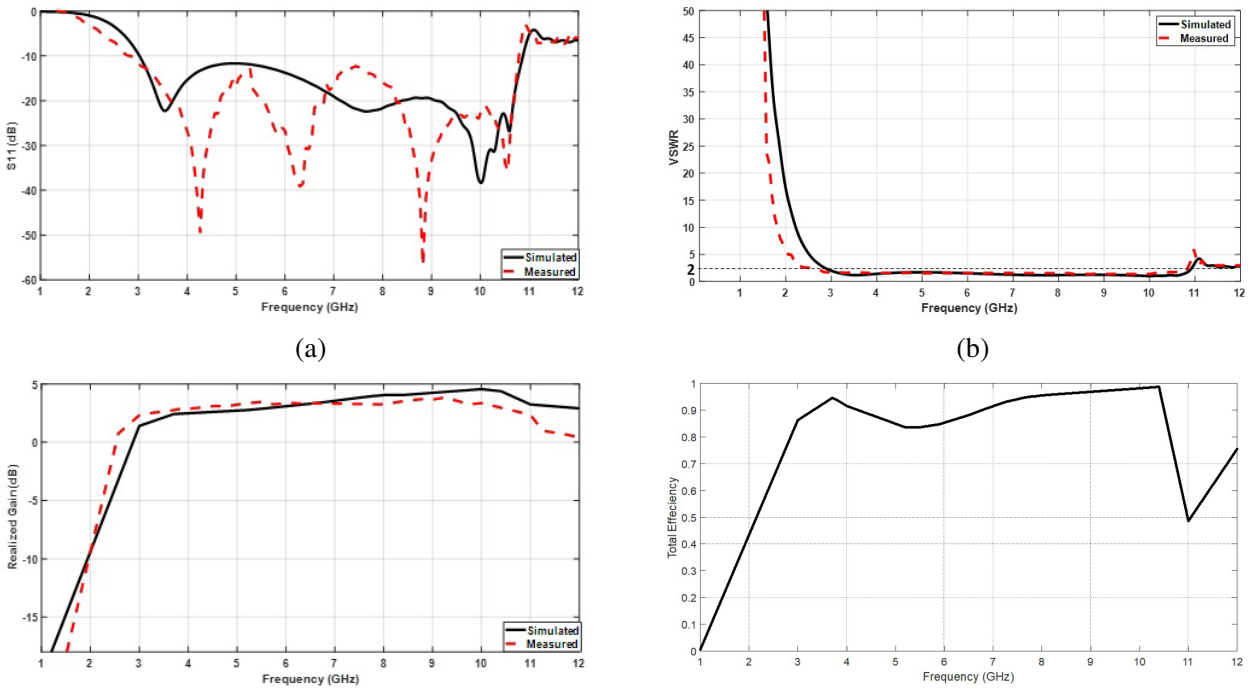

(a) (b) (c) (d)

Figure 12. Simulated and measured of the proposed UWB filtenna (state 1). (a) Reflection coefficients (S_{11}). (b) VSWR values. (c) Realized gains. (d) Simulated total efficiency.

with a fractional bandwidth 136.85% (143.69%). The VSWR (shown in Figure 12(b)) has values less than 2 across the entire UWB passband. The simulated (measured) realized gain in Figure 12(c) has values between 1.3 dBi and 4.5 dBi within the passband of the filtenna. As shown in Figure 12(d), the simulated total efficiency of the filtenna is greater than 89% across all passbands in this state.

Figure 13(a) shows the surface current flowing toward the patch element at a frequency of 5.5 GHz. In addition, this Figure also shows that the π-shaped resonators are ineffective in the antenna passband. Also, Figure 13(b) depicts how the current passes through the antenna feeding directly to the radiating patch element at a frequency of 7.6 GHz, implying that there is no effect on the antenna passband. As a result, the filtenna operates at UWB without any band notch.

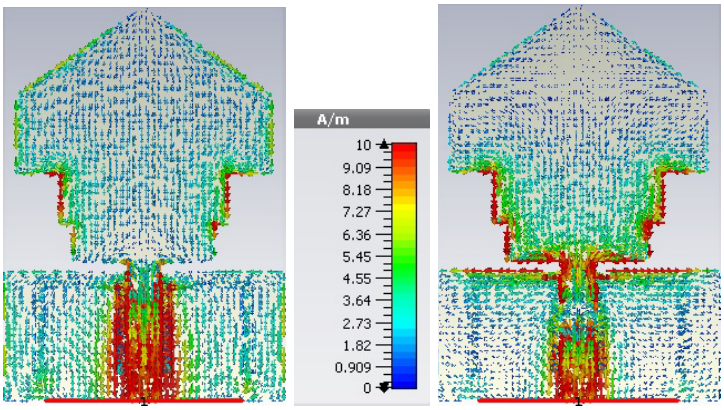

(a) (b)

Figure 13. Simulated surface current of the filtenna (state 1) at (a) 5.5 GHz, (b) 7.6 GHz.

3.2. State 2: (All PIN Diodes Are ON)

In this state, the diodes act as conductors between the two segments of the π-shaped resonators. The current flowing in a pair of π-shaped resonators results in a structure acting like a complete coupled stopband filter with a center frequency of 5.5 GHz. This structure operates as a half-wavelength band notch filter that insures the cancelation of the 5G WLAN applications. Figure 14(a) shows the simulated (measured) reflection coefficient with a value of -0.9 dB (-0.7 dB) at the notched frequency to cancel the interference with the 5G WLAN band. The simulated (measure) VSWR is less than 2 across all passbands of filtenna except at a notched frequency which is 19.128 (20.17) as shown in Figure 14(b). The value of the realized gain is greater than 2 dBi within the entire UWB of filtenna except at a notched frequency, which is about -13.72 dBi (-14.61 dBi) as shown in Figure 14(c). The simulated total efficiency of the filtenna in this state is greater than 90% except at the notch frequency which is reduced to 9% as illustrated in Figure 14(d). As a result, the band notch guarantees the elimination of the radiation of 5.466 GHz (5.7 GHz).

Figure 15 shows the surface current distribution of the filtenna at frequencies of 5.5 GHz and 7.6 GHz, respectively. Figure 15(a) depicts how the current is concentrated at the π-shaped resonator at a frequency of 5.5 GHz, which cancels out the interference with the 5G WLAN band, whereas Figure 15(b) depicts how the current passes through the antenna feeding directly to the radiating patch element at a frequency of 7.6 GHz, implying that there is no effect on the antenna passband.

3.3. State 3: (All PIN Diodes Are OFF)

In this state, the diodes act as insulators that cut the current flow in all resonators. Therefore, the passband of the filtenna is not affect by the π-shaped resonators, while the open stub quarter-wavelength resonator that is located inside the feed line of the antenna acts as a stopband filter to eliminate the radiation of 7.545 GHz (7.48 GHz). The simulated (measured) reflection coefficient (S_{11}) at the notched frequency is -0.858 dB (-0.4 dB), and the VSWR is greater than 20 (47) while the realized gain is

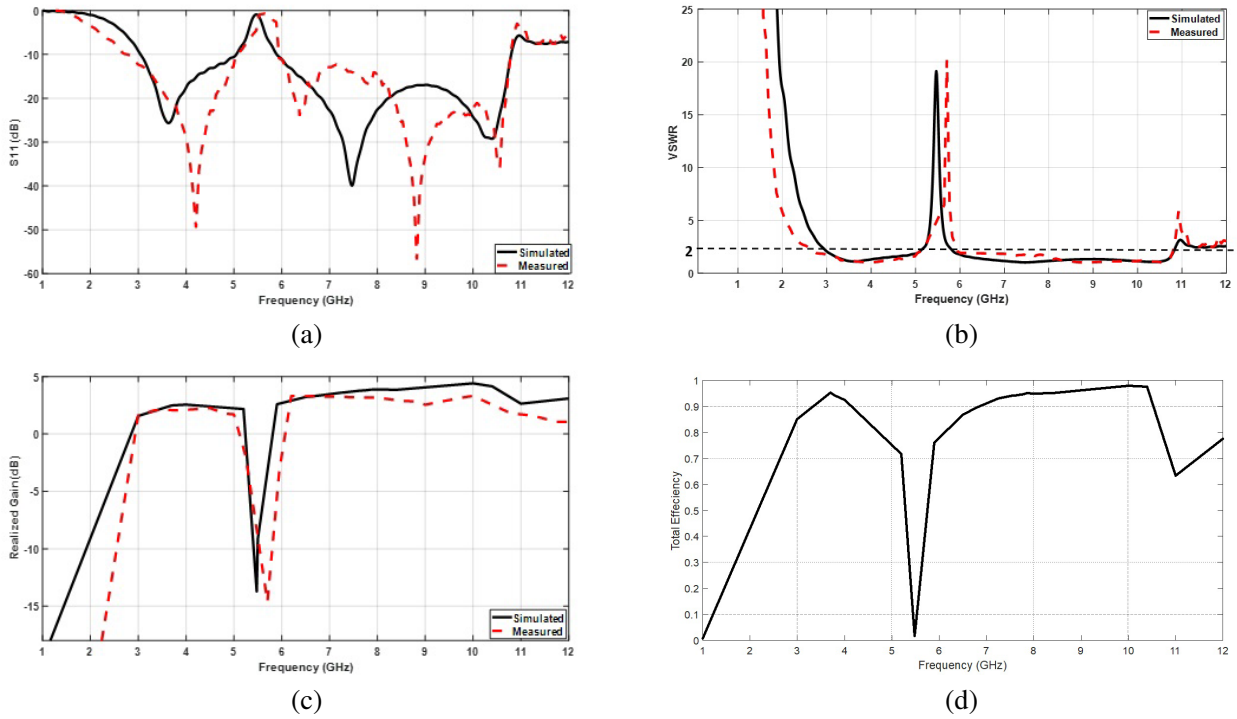

Figure 14. Simulated and measured of the proposed UWB filtenna (state 2). (a) Reflection coefficients (S_{11}). (b) VSWR values. (c) Realized gains. (d) Simulated total efficiency.

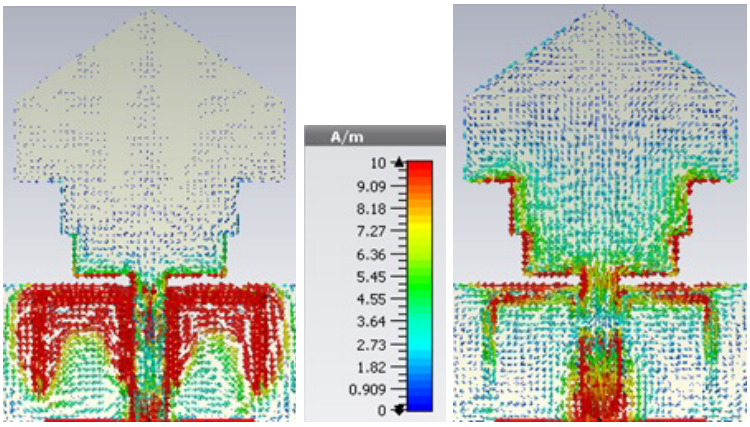

Figure 15. Simulated surface current of the filtenna (state 2) at (a) 5.5 GHz (b) 7.6 GHz.

−10 dBi (−14 dBi) as shown in Figures 16(a), (b), and (c), respectively. The simulated total efficiency of the filtenna as given in Figure 16(d) shows that it is greater than 90% across the entire passband except at the notched frequency, which is reduced to 21.27%.

Figure 17(a) depicts the surface current flowing toward the patch element at a frequency of 5.5 GHz. In addition, this figure also shows that the π-shaped resonators are ineffective in the antenna passband. On the other hand, the current is centered at the quarter wavelength inside the antenna's feed line. There is no current passing to the radiating patch element at a frequency of 7.6 GHz, and this indicates the presence of the stopband filter, as shown in Figure 17(b). As a result, the interference with the X-band is almost perfectly canceled.

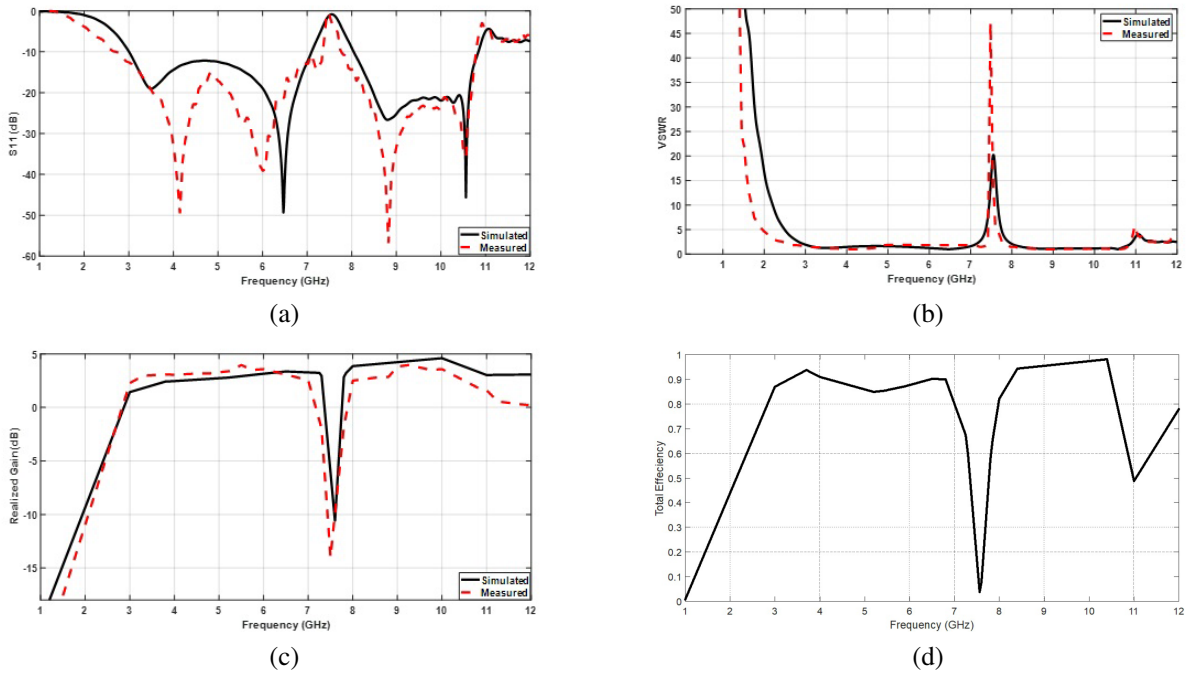

Figure 16. Simulated and measured of the proposed UWB filtenna (state 3). (a) Reflection coefficients (S_{11}). (b) VSWR values. (c) Realized gains. (d) Simulated total efficiency.

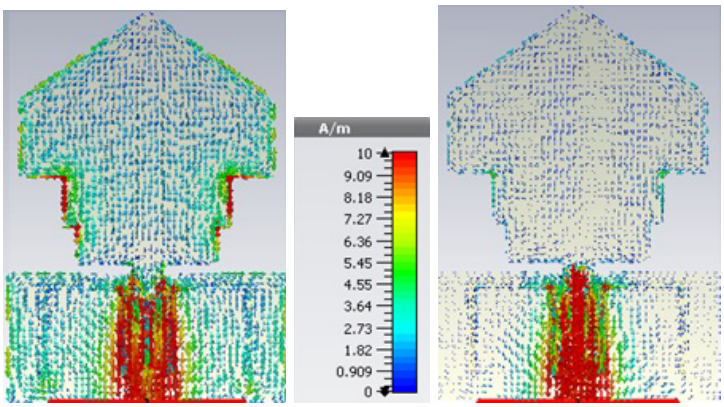

Figure 17. Simulated surface current of the filtenna (state 3) at (a) 5.5 GHz, (b) 7.6 GHz.

3.4. State 4: (D_{1A} and D_{1B} Are ON While D_2 Is OFF)

In this state, both band notch elements are active to cancel the interference with the 5G WLAN and X-band satellite downlink. In other words, dual-band notches centered at 5.466 GHz and 7.578 GHz (5.6 GHz and 7.55 GHz) exist within the passband of the filtenna. The simulated (measured) reflection coefficients (S_{11}) at the first and second notched frequencies are -0.88 dB (-0.94 dB) and -0.817 dB (-0.4 dB) as shown in Figure 18(a). The simulated (measured) VSWR as plotted in Figure 18(b) shows that it is greater than 20 (21) and 19 (47) at the notched frequencies. The values of simulated (measured) realized gains are reduced to -14.4 dBi (-11.92 dBi) and -9.22 dBi (-15.15 dBi) at the dual notched frequencies as shown in Figure 18(c).

Figure 18(d) shows that the simulated total efficiency of the filtenna is greater than 90% across the

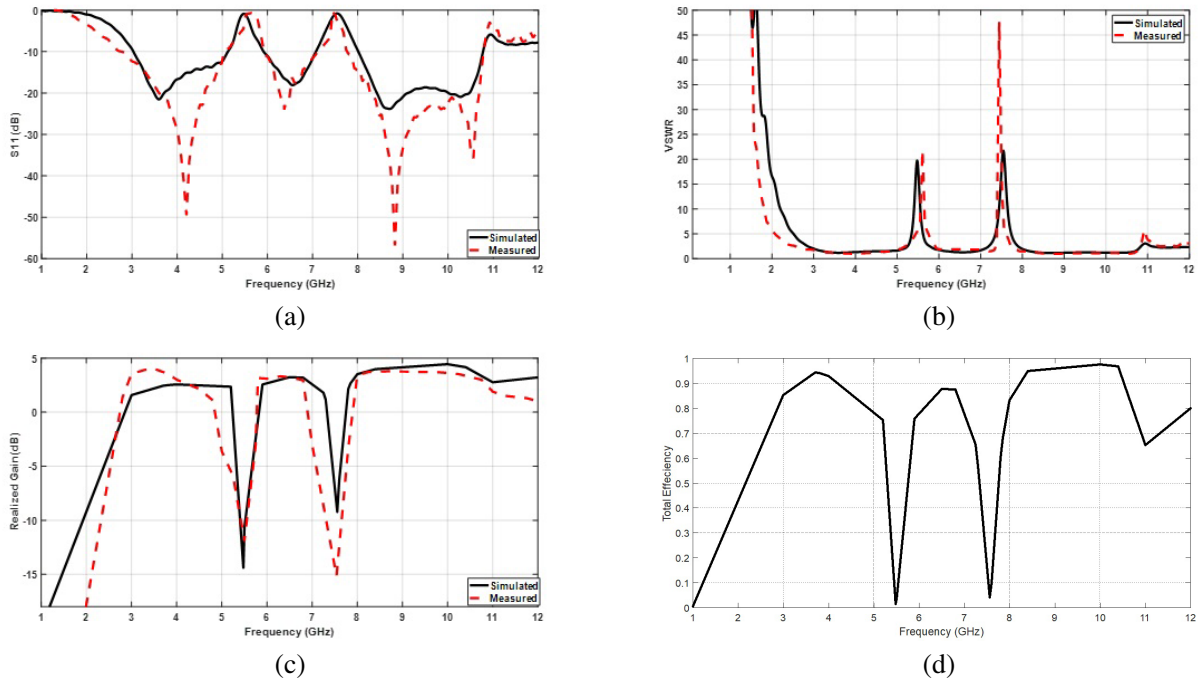

Figure 18. Simulated and measured of the proposed UWB filtenna (state 4). (a) Reflection coefficients (S_{11}). (b) VSWR values. (c) Realized gains. (d) Simulated total efficiency.

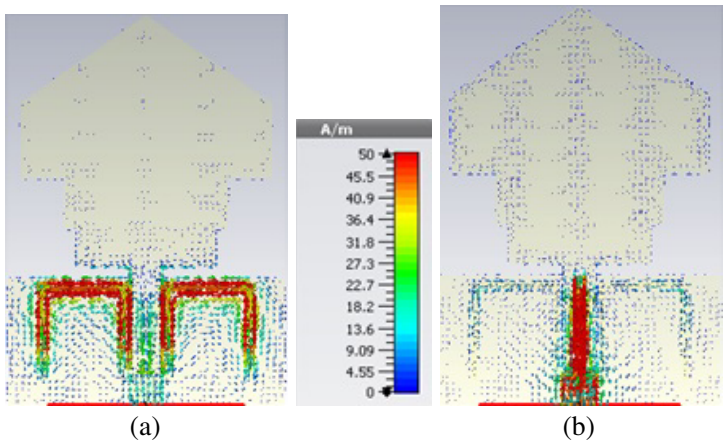

Figure 19. Simulated surface current of the filtenna (state 4) at (a) 5.5 GHz, (b) 7.6 GHz.

entire passband except at the notched frequencies, which are reduced to 8.5% and 24.2%, respectively.

Figure 19(a) depicts how current is concentrated at the π-shaped resonator at 5.5 GHz to cancel out the interference with the 5G WLAN. In addition, the current is centered at the quarter wavelength resonator that is located inside the feed line of the filtenna, and there is no current passing through it to the radiating patch at a frequency of 7.6 GHz. This means that there is a stopband filtering at this frequency as shown in Figure 19(b). As a result, the interference with the 5G WLAN and X-band is almost perfectly canceled. All the simulated and measured data for the four states of the proposed UWB filtenna are listed in Table 3.

Figure 20 shows the simulated and measured power patterns of the filtenna in the E-plane (YOZ plane) and H-plane (XOZ plane) at the frequencies of 3.5 GHz, 7.6 GHz, and 10 GHz. The realized gain of the filtenna was used to calibrate the power patterns. The H-plane shows omnidirectional radiation

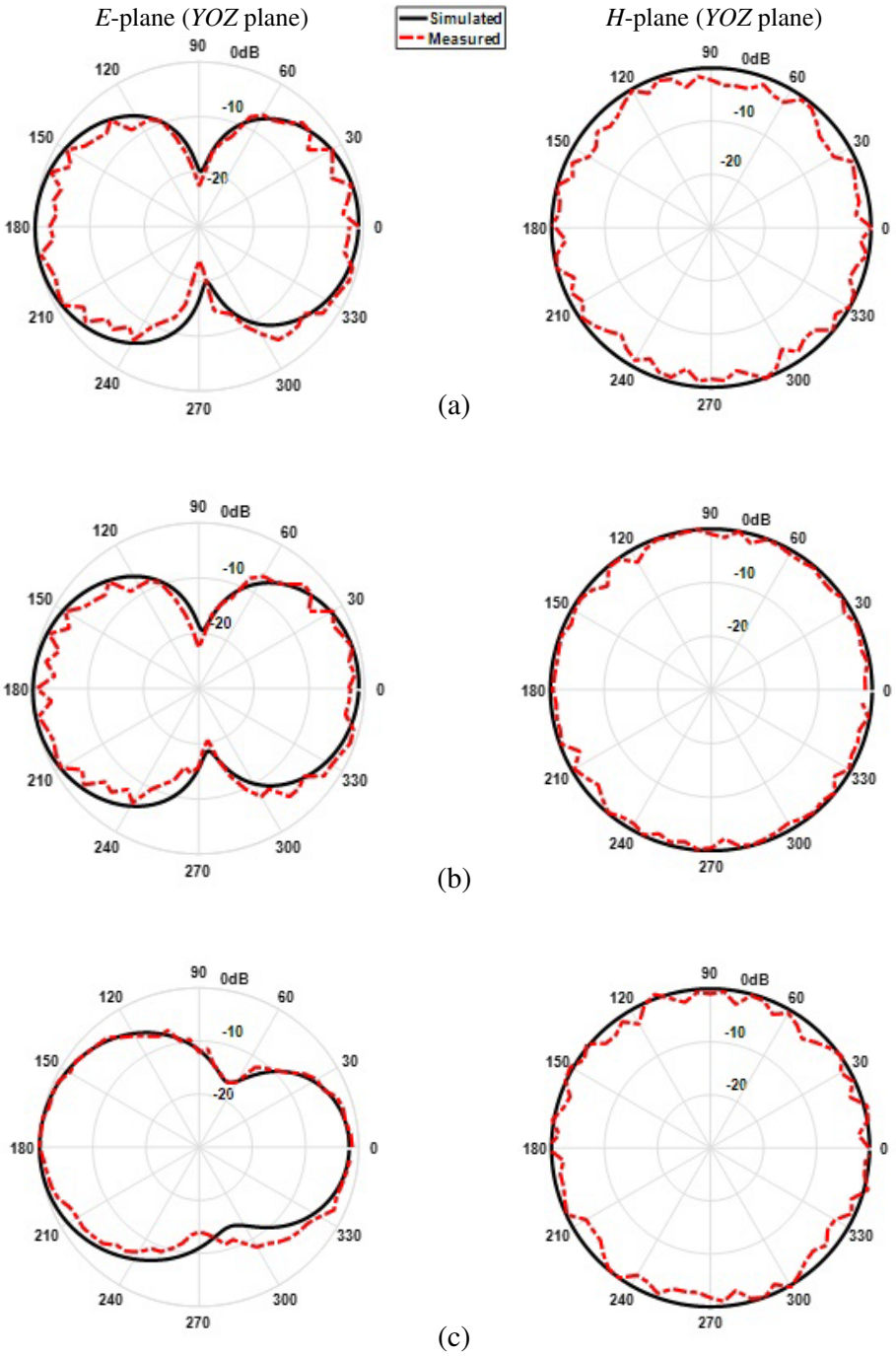

Figure 20. Power patterns of the UWB filtenna (a) 3.5 GHz, (b) 7.6 GHz, (c) 10 GHz at state 1 without any band notch.

patterns at all three frequencies, which implies that the filtenna radiates in all directions regardless of its orientation. On the other hand, the filtenna has bidirectional power patterns in the *E*-plane except for slight distortion at the higher frequency of 10 GHz.

Table 4 compares the proposed reconfigurable UWB filtenna specifications with some previous works, which have dual notched bands. The advantages of the proposed filtenna over the other designs are its compact size, high VSWR at the notched bands, and lower reflection coefficient, good rejection, and lower realized gain values at the notched frequencies.

Table 3. The results of the filtenna in different cases of PIN switch diodes.

State	D_{1A} & D_{1B}	D_2	Results	Passband (GHz)	Notch Band Characteristics					
					Notched band (GHz)	f_n (GHz)	Rejection S_{11} (dB)	Gain (dBi) @ f_n	VSWR	Rad. Eff.%
1	OFF	ON	Sim.	3.024–10.87	None Full UWB	None Full UWB	None	4.5	2	89
1	OFF	ON	Mea.	2.825–10.74	None Full UWB	None Full UWB	None	4.2	2	-
2	ON	ON	Sim.	3.046–10.79	5.07–5.92 (5G WLAN)	5.466	–0.9	–13.72	19.13	9
2	ON	ON	Mea.	2.768–10.88	5.02–6	5.7	–0.7	–14.61	20.17	-
3	OFF	OFF	Sim.	3.01–10.84	7.12–8 (X-Band)	7.545	–0.858	–10	20.25	21.27
3	OFF	OFF	Mea.	2.7–10.76	7.38–7.743	7.48	–0.4	–14	47.18	-
4	ON	OFF	Sim.	3.03–10.77	5.14–5.9 & 7.07–8	5.466 & 7.578	–0.88 & –0.817	–14.14 & –9.22	20.25 & 19	8.5 & 24.2
4	ON	OFF	Mea.	2.77–10.741	5.05–5.86 & 7.2–7.75	5.6 & 7.55	–0.94 & –0.4	–11.92 & –15.15	21.79 & 47.65	-

Table 4. Comparison of the proposed filtenna with other related works.

Ref.	No. of switches	Passband (GHz)	Notch frequency f_n (GHz)	S_{11} @ f_n (dB)	Gain @ f_n (dBi)	VSWR @ f_n	Size (mm)
[7]	4PIN diodes	3.06–10.67 3.07–0.9	i. None band notch ii. 5.25 and 5.8	None −1.7	5.8 −5	N/A	33.8 × 30
[12]	2PIN diodes	3–10	i. 3.8 & 5.2 ii. 3.8 and 5.56	−4 −3.7	N/A	N/A	65 × 70
[14]	4PIN diodes	3–11	i. 5.4 ii. 7.2	N/A	−2 −6	12 17	26 × 28
[34]	2PIN diodes	2.65–14.56	i. 5.457 & 3.52 ii. 5.57 iii. 3.52 iv. None band-notch	> -10	−1 −5	N/A	40 × 30
[35]	3PIN diodes	3.1–13	i. None band-notch ii. (5.1–5.7) iii. (7.2–7.8) iv. (5.1–5.7) & (7.2–7.8)	N/A	- −4 −6	< 2 5 6	30.3 × 24.8
This work	3PIN diodes	2.825–10.74	i. None (Full UWB) ii. 5.7 (5.2–6) iii. 7.48 (7.38–7.743) iv. 5.6 (5.05–5.86) & 7.55 (7.2–7.75)	None −0.7 −0.4 −0.94 & −0.4	4.2 −12 −14 −11.92 & −14	< 2 > 20 > 47 > 21 & > 47	31 × 22

4. CONCLUSION

In this paper, a compact UWB filtenna with reconfigurable and sharp dual-band notches for underlay cognitive radio (CR) has been successfully presented. A printed UWB filtenna was successfully designed and fabricated, which includes a UWB antenna and a reconfigurable stopband filter. For filter reconfigurability, three PIN diodes are used. Four states are obtained from these three diodes depending on the status of PIN diodes. A full UWB coverage is achieved when a pair of PIN diodes (D_{1A}, D_{1B}) are turned OFF while D_2 is turned ON. A UWB with a single notch band has been realized at a range of (5.02–6) GHz to cancel the interference with 5G WLAN applications when all PIN diodes are turned ON. A UWB with a single notch band of X-band satellite downlink at a frequency range of (7.38–7.743) GHz is fulfilled when all PIN diodes are turned OFF. Finally, a UWB with a dual-band notch is achieved to cancel the interference with 5G WLAN and X-band satellite downlink when (D_{1A}, D_{1B}) are turned ON while D_2 is turned OFF. The realized gain is found to be 4.5 dBi within the passband except in the notched frequencies, while it decreases to less than −11 dBi at the notched frequency. The simulated and measured results demonstrate that the filtenna has a low reflection coefficient (S_{11}) and sharp VSWR at the notched frequencies which means an excellent band rejection behavior.

REFERENCES

1. FCC, "First report and order on ultra-wideband technology," FCC, Washington, DC, USA, 2002.
2. Panda, J. R., P. Kakumanu, and R. S. Kshetrimayum, "A wide-band monopole antenna in combination with a UWB microwave band-pass filter for application in UWB communication system," *2010 Annual IEEE India Conference (INDICON)*, 1–4, 2010.
3. Federal Communications Commission, "Revision of part 15 of the commission's rules regarding ultra-wideband transmission systems: First report and order," FCC-02, 2002.
4. Fallahi, R., A. A. Kalteh, and M. Roozbahani, "A novel UWB elliptical slot antenna with band-notched characteristics," *Progress In Electromagnetics Research*, Vol. 82, 127–136, 2008.
5. Liu, H.-W., C.-H. Ku, T.-S.Wang, and C.-F. Yang, "Compact monopole antenna with band-notched characteristic for uwb applications," *IEEE Antennas and Wireless Propagation Letters*, Vol. 9, 397–400, 2010.
6. Nguyen, T. D., D. H. Lee, and H. C. Park, "Design and analysis of compact printed triple bandnotched uwb antenna," *IEEE Antennas and Wireless Propagation Letters*, Vol. 10, 403–406, 2011.
7. Ahmad, W. and D. Budimir, "Reconfigurable UWB filtennas with sharp wlan dual bandnotch," *2015 European Microwave Conference (EuMC)*, 1228–1231, IEEE, 2015.
8. Li, W. T., Y. Q. Hei, W. Feng, and X. W. Shi, "Planar antenna for 3G/bluetooth/WiMax and UWB applications with dual band-notched characteristics," *IEEE Antennas and Wireless Propagation Letters*, Vol. 11, 61–64, 2012.
9. Tang, T.-C. and K.-H. Lin, "An ultrawideband mimo antenna with dual band-notched function," *IEEE Antennas and Wireless Propagation Letters*, Vol. 13, 1076–1079, 2014.
10. Lin, Y.-C. and K.-J. Hung, "Compact ultrawideband rectangular aperture antenna and bandnotched designs," *IEEE Transactions on Antennas and Propagation*, Vol. 54, No. 11, 3075–3081, 2006.
11. Lui, W., C. Cheng, and H. Zhu, "Compact frequency notched ultra-wideband fractal printed slot antenna," *IEEE Microwave and Wireless Components Letters*, Vol. 16, No. 4, 224–226, 2006.
12. Tawk, Y., J. Costantine, and C. G. Christodoulou, "Reconfigurable filtennas and MIMO in cognitive radio applications," *IEEE Transactions on Antennas and Propagation*, Vol. 62, No. 3, 1074–1083, 2013.
13. Lin, C.-C., P. Jin, and R. W. Ziolkowski, "Single, dual and tri-band-notched ultrawideband (UWB) antennas using capacitively loaded loop (CLL) resonators," *IEEE Transactions on Antennas and Propagation*, Vol. 60, No. 1, 102–109, 2011.
14. Alnahwi, F., A. Abdulhameed, H. Swadi, and A. Abdullah, "A compact wide-slot UWB antenna with reconfigurable and sharp dual-band notches for underlay cognitive radio applications," *Turkish Journal of Electrical Engineering & Computer Sciences*, Vol. 27, No. 1, 94–105, 2019.
15. Yoon, I.-J., H. Kim, H. Yoon, Y. Yoon, and Y.-H. Kim, "Ultra-wideband tapered slot antenna with band cutoff characteristic," *Electronics Letters*, Vol. 41, No. 11, 629–630, 2005.
16. Zhu, F., S. Gao, A. T. Ho, R. A. Abd-Alhameed, C. H. See, T. W. Brown, J. Li, G. Wei, and J. Xu, "Multiple band-notched UWB antenna with band-rejected elements integrated in the feed line," *IEEE Transactions on Antennas and Propagation*, Vol. 61, No. 8, 3952–3960, 2013.
17. Jaglan, N., B. Kanaujia, S. D. Gupta, and S. Srivastava, "Triple band notched UWB antenna design using electromagnetic band gap structures," *Progress In Electromagnetics Research C*, Vol. 66, 139–147, 2016.
18. Kollipara, V., S. Peddakrishna, and J. Kumar, "Planar EBG loaded UWB monopole antenna with triple notch characteristics," *International Journal of Engineering and Technology Innovation*, Vol. 11, No. 4, 294, 2021.
19. Chen, H., Y. Ding, and D. S. Cai, "A CPW-fed UWB antenna with WiMAX/WLAN band-notched characteristics," *Progress In Electromagnetics Research Letters*, Vol. 25, 163–173, 2011.

20. Abbas, A., N. Hussain, J. Lee, S. G. Park, and N. Kim, "Triple rectangular notch UWB antenna using EBG and SRR," *IEEE Access*, Vol. 9, 2508–2515, 2020.
21. Rekha, V. S. D., P. Pardhasaradhi, B. T. P. Madhav, and Y. U. Devi, "Dual band notched orthogonal 4-element mimo antenna with isolation for UWB applications," *IEEE Access*, Vol. 8, 145 871–145 880, 2020.
22. Tawk, Y., J. Costantine, and C. Christodoulou, "A varactor-based reconfigurable filtenna," *IEEE Antennas and Wireless Propagation Letters*, Vol. 11, 716–719, 2012.
23. Kataria, T. K., M. Bastida, J. R. Reyes-Ayona, J. L. O. Cervantes, and A. Corona-Chavez, "Planar differential filtenna for communications," *Progress In Electromagnetics Research Letters*, Vol. 79, 33–38, 2018.
24. Hu, K.-Z., M.-C. Tang, D. Li, Y. Wang, and M. Li, "Design of compact, single-layered substrate integrated waveguide filtenna with parasitic patch," *IEEE Transactions on Antennas and Propagation*, Vol. 68, No. 2, 1134–1139, 2019.
25. Hosain, M. M., S. Kumari, and A. K. Tiwary, "Compact filtenna for wlan applications," *Journal of Microwaves, Optoelectronics and Electromagnetic Applications*, Vol. 18, 70–79, 2019.
26. Ahmad, W., "Integrated filter antennas for wireless transceivers," Ph.D. Dissertation, University of Westminster, 2017.
27. Haraz, O. and A.-R. Sebak, "UWB antennas for wireless applications," *Advancement in Microstrip Antennas with Recent Applications*, 125–152, 2013.
28. Azenui, N. C. and H. Yang, "A printed crescent patch antenna for ultrawideband applications," *IEEE Antennas and Wireless Propagation Letters*, Vol. 6, 113–116, 2007.
29. Balanis, C. A., *Antenna Theory: Analysis and Design*, John Wiley & Sons, 2015.
30. Hong, J.-S. G. and M. J. Lancaster, *Microstrip Filters for RF/Microwave Applications*, John Wiley & Sons, 2004.
31. ADS, "Advanced design system," 2021.
32. CST, "Computer simulation technology based on fit method," 2017.
33. Skyworks Solutions, Available online at: https://www.skyworksinc.com/-/media/938aa8a86545442389dadffbee0e2741.ashx.
34. Alhegazi, A., Z. Zakaria, N. A. Shairi, M. I. Ibrahim, and S. Ahmed, "A novel reconfigurable UWB filtering-antenna with dual sharp band notches using double split ring resonators," *Progress In Electromagnetics Research C*, Vol. 79, 185–198, 2017.
35. Oraizi, H. and N. V. Shahmirzadi, "Frequency-and time-domain analysis of a novel UWB reconfigurable microstrip slot antenna with switchable notched bands," *IET Microwaves, Antennas & Propagation*, Vol. 11, No. 8, 1127–1132, 2017.